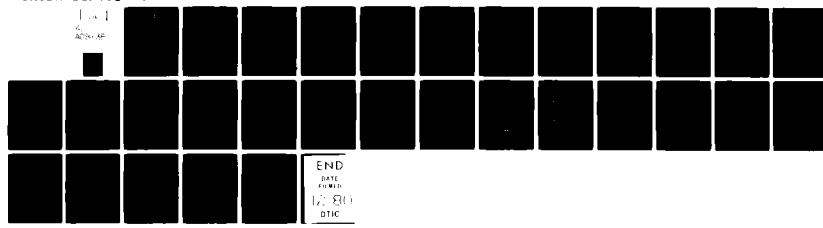


AD-A091 638 NORTHWESTERN UNIV. EVANSTON ILL MATERIALS RESEARCH CENTER F/G 11/9  
THERMALLY STIMULATED DISCHARGE CURRENTS FROM SODIUM NITRATE-DOPED  
SEP 80 H UEDA, S H CARR N00014-75-C-0963

UNCLASSIFIED NL

TR-9



END  
17-80  
DTIC

*f*  
**LEVEL**

12

"THERMALLY STIMULATED DISCHARGE CURRENTS  
FROM SODIUM NITRATE-DOPED POLYACRYLONITRILE"

by

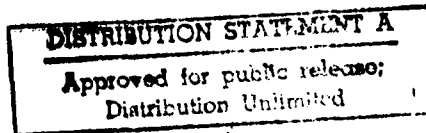
H. Ueda and S. H. Carr

Department of Materials Science and Engineering  
and  
Materials Research Center  
Northwestern University  
Evanston, IL 60201

Submitted for publication to  
Journal of Macromolecular Science-Physics



August 1980



**DDC FILE COPY**

80 9 29 057

SECURITY CLASSIFICATION OF THIS PAGE (When Data Entered)

REPORT DOCUMENTATION PAGE		READ INSTRUCTIONS BEFORE COMPLETING FORM
1. REPORT NUMBER Technical Report No. 9	2. GOVT ACCESSION NO. AD-A091	3. RECIPIENT'S CALL NUMBER 638 Electrical report
4. TITLE (If different from block 1) THERMALLY STIMULATED DISCHARGE CURRENTS FROM SODIUM NITRATE-DOPED POLYACRYLONITRILE <sup>6</sup>	5. TYPE OF REPORT/PERIOD COVERED Interim <sup>9</sup>	6. PERFORMING ORG. REPORT NUMBER 9
7. AUTHOR(s) H. Ueda & S. H. Carr <sup>10</sup>	8. CONTRACT OR GRANT NUMBER(s) N00014-75-C-0963 <sup>11</sup>	10. PROGRAM ELEMENT, PROJECT, TASK AREA & WORK UNIT NUMBERS NR 051-599
9. PERFORMING ORGANIZATION NAME AND ADDRESS Materials Research Center and Department of Materials Science and Engineering Northwestern University, Evanston, IL 60201	11. CONTROLLING OFFICE NAME AND ADDRESS ONR Branch Office 536 S. Clark Street, Chicago, IL 60605 <sup>12</sup>	12. REPORT DATE September 3, 1980 <sup>13</sup>
14. MONITORING AGENCY NAME & ADDRESS (if different from Controlling Office)		13. NUMBER OF PAGES 29
		15. SECURITY CLASS. (of this report) Unclassified
		15a. DECLASSIFICATION/DOWNGRADING SCHEDULE
16. DISTRIBUTION STATEMENT (of this Report) See appended distribution list.		
17. DISTRIBUTION STATEMENT (of the abstract entered in Block 20, if different from Report)		
18. SUPPLEMENTARY NOTES		
19. KEY WORDS (Continue on reverse side if necessary and identify by block number) Electrets, polyacrylonitrile, Thermally Stimulated Discharge Current (TSDC), ion-doping, dielectrics, space charges, electrical conductivity.		
20. ABSTRACT (Continue on reverse side if necessary and identify by block number) Enhancement of charge capable of being stored in a polymer by direct incorporation of ions has been studied. The system chosen was polyacrylonitrile (PAN) into which had been dissolved either sodium nitrate, ammonium nitrate, or lithium chloride. Stored charge was measured by use of the Thermally Stimulated Discharge Current (TSDC) method. It was found, for example, that addition of 4 wt% salt could enhance stored charge by at least fifty-fold. The TSDC method also revealed that the stored charge arose from at least six identifiable contributions. The lower temperature contributions involved (contd.)		

20. Abstract (contd).

preferentially oriented dipoles, while the higher-temperature ones were caused by displaced real charges. No evidence for a strong interaction between dissolved ionic species and PAN chains at the repeat unit level was found, but density fluctuations on the supramolecular size-scale do appear to influence the stability of these stored real charges.

"THERMALLY STIMULATED DISCHARGE CURRENTS  
FROM SODIUM NITRATE-DOPED POLYACRYLONITRILE"

INTRODUCTION

Interest in polymer films possessing stable and high levels of electrical polarization (electrets) has remained high in recent years because such materials exhibit pyro- and piezoelectric behavior. Since the time of the early work on polyvinylidene fluoride films (1), the picture has emerged that electrical polarization arises from both a preferred orientation of dipoles and some distribution of real charges across the thickness of these films. These charges are likely carried as ions on small, non-polymeric molecules or on individual and unbound atoms. In general, all polymer films contain some amount of small molecules, e.g., catalyst, plasticizer, and ions produced by dissociation, solvent, or moisture. These small molecules have an effect upon both the state of macromolecules in solids and the properties possessed by these solids. Some molecular motion is enhanced, and some molecular motion is diminished by the presence of these small molecules in polymers (2-4). These phenomena are dependent upon the interaction between repeat units in the polymer and these small molecules.

Since Bucci, et al., (5,6) advanced the Thermally Stimulated Discharge Current (TSDC) method, it has been widely applied to the investigation of such polymer electrets (see, for example, refs. 7 and 8). Because TSDC data contain a wealth of information on relaxation processes of both dipoles and space charges measured at very low ( $<10^{-2}$  Hz) effective frequencies (9), they are capable of resolving individual relaxation processes from one another (7).

In this paper, the effect of  $\text{NaNO}_3$  doping on the TSDC of polyacrylonitrile (PAN) is reported. Mechanical properties (4,10,11) and dielectric properties (12-15) of PAN have been investigated by many authors, but the exact under-

standing about the relaxational and dispersion phenomena of PAN has not been achieved. Comstock, et al., (16) observed TSDC peaks at 90 and 180°C in polyacrylonitrile (PAN) poled with a field of  $7 \times 10^4$  V/cm at 130°C. They attributed the peaks at 90 and 180°C to the reorientation of nitrile dipoles in paracrystalline region and to microscopic charge displacement, respectively. Stupp and Carr (17) proposed that the current peak at 190°C could be associated somehow with relaxation of chain backbone segments; it was also revealed that TSDC in the high temperature ranges might reflect the onset of pyrolytic chemical degradation events.

Accession No.	
NTIS CR&RL	<input checked="" type="checkbox"/>
DTIC TAB	<input type="checkbox"/>
Unpublished	<input type="checkbox"/>
Justification	Per 26-102
Data 7 Oct 80	
By	On file
Distribution	
Availability Codes	
Dist	Avail and/or Special
A	

EXPERIMENTAL

PAN was supplied by the Standard Oil Company (Ohio), Cleveland, Ohio. The material is reported to have a weight average molecular weight in excess of 35,000. Purification involved the following: PAN powder was first dissolved in dimethyl formamide (DMF) at a concentration of 5 wt%, and then it was reprecipitated by pouring into distilled methanol. Purified PAN in 2% dimethyl formamide (DMF) solutions was first poured on a glass surface. Solvent evaporation was done under reduced pressure for 24 hours at room temperature, and then these cast films were dried under vacuum for 24 hours at 40° C. Gold was vacuum-evaporated onto each side of the sample to serve as electrodes (diameter is 1.5 cm). PAN films doped with either NaNO<sub>3</sub>, NH<sub>4</sub>NO<sub>3</sub>, or LiCl were prepared by first dissolving the salt in DMF and subsequently adding it dropwise to the PAN solution in DMF. Thickness of the samples ranged from 30 to 54 μm. Dimensions of the film samples prepared for TSDC measurements were squares, 25 mm by 25 mm.

TSDC thermograms and direct current (dc) conductivity were recorded with an Electret Thermal Analyzer (Toyo-Seiki, Seisaku-Sho, Ltd.). All measurements were made with a heating rate of 2° C/min. Samples for TSDC measurement were held for 30 min. under the imposed electrical field at 130° C, unless otherwise noted. Samples were subsequently cooled under the applied field to -150° C. Depolarization currents were recorded in the range from -100 to 190° C. A charge amplifier and a functional generator (Kikusui Electronics Corp.) were used to measure dielectric constants at 11 Hz.

Salt concentrations are expressed in moles per gram of PAN polymer. In equivalent units, one finds, for example,  $1 \times 10^{-4}$  moles NaNO<sub>3</sub>/gm PAN equals PAN 0.85 wt% in NaNO<sub>3</sub> or  $5.3 \times 10^{-3}$  moles NaNO<sub>3</sub>/AN repeat unit.

RESULTS

TSDC thermograms of  $\text{NaNO}_3$ -doped PAN are shown in Figures 1 and 2. Figure 2 is a scale expansion of the temperature range,  $0^\circ\text{C}$  to above  $100^\circ\text{C}$ , revealing interesting structure of some significance to the study in question. Although it is difficult to track exactly how the various peaks seen in these thermograms grow or shift with salt concentration, it is believed that a  $\text{NaNO}_3$  concentration-dependence of these peaks is shown by the curves in Figure 3. Somewhat arbitrarily, and for the purposes of this paper only, we have assigned identification symbols to these peaks as indicated in Figure 3. It appears that only the  $\delta$  peak exhibits appreciable salt concentration dependence, while all other peaks exhibit a salt-concentration independence. Basically, what is seen are peaks in undoped PAN at  $-50^\circ\text{C}$  ( $\delta$  peak),  $100^\circ\text{C}$  ( $\gamma_1$  peak), and  $\geq 170^\circ\text{C}$  ( $\alpha$  peak). The peaks occurring around  $100^\circ\text{C}$  and  $170^\circ\text{C}$  have been reported<sup>16,17</sup>, while the peak around  $-50^\circ\text{C}$  has not been reported previously. Peaks observed above  $0^\circ\text{C}$  have maximum peak currents,  $I_{\max}$ , that are strongly dependent on  $\text{NaNO}_3$  concentration.

Because of the difficulty in making clear definition of peaks in various temperature ranges, it has been necessary to look at charges associated with the various peaks and to look at the activation energy spectrum throughout the temperature region in question. Figure 4 shows charge released during TSDC runs at temperatures above  $70^\circ\text{C}$ . This is the range dominated heavily by the presence of mobile ionic species which contribute a space charging to these films. It is interesting to note that addition of ionic species much above 1 wt%  $\text{NaNO}_3$  fails to result in an accompanying increase in charging. It is possible that this indicates the onset of ionic clustering in these higher concentration regions. Such a characteristic would allow the film to accommodate the dopant but not have the dopant species actually contributing

mobile ionic charges throughout the material itself. Use of peak cleaning and partial heating methods<sup>7</sup> yields TSDC data from which one can calculate activation energy for the depolarization process prevailing at successively higher temperatures.

Results of such studies on undoped PAN and on  $\text{NaNO}_3$ -doped PAN are shown in Figure 5. Here, one sees the maximum in the activation energy distribution being coincident with the  $\gamma_1$  peak. Above this temperature range, activation energy for the depolarization process actually declines, indicating that higher levels of thermal energy are available to facilitate transport of charges, as is a condition consistent with the proposition that depolarization in these higher temperature ranges is due to the neutralization of space charge polarization. On the lower temperature side of the activation energy maximum, one sees a more-or-less continuous fall-off of activation energy for undoped films. The values of activation energy, as they diminish, become increasingly consistent with their being associated with local-mode individual molecular relaxation processes. The small, but distinct, plateau in activation energy for the  $\text{NaNO}_3$ -doped material in the temperature range  $35^\circ$  rather clearly implicates some specific molecular process of as-yet unidentified origin that is probably responsible for the  $\gamma_3$  peak.

Figure 6 represents TSDC thermograms of both  $\text{NH}_4\text{NO}_3$ - and LiCl-doped PAN. The released charge of the  $\delta$  peak,  $\gamma_3$  peak, and charge ( $Q$ ) above  $70^\circ\text{C}$  for each sample are listed in Table I. Charge released from the  $\delta$  peak may be taken as being independent of the kind of ionic species doped into the PAN, but a difference can be clearly seen in  $I_{\max}$  for many of the peaks at higher temperatures in the thermograms. Depolarization current reversal for the specimen, N-2, remains a mystery but is, nevertheless, reproducible. It is plausible that such an effect is related to some chemical reaction in which ammonium ions may be a participating species.

### DISCUSSION

Data presented in Figures 1 through 6 reveal that ion-doping of PAN greatly enhances the charge this polymer can store. Further, one can infer that the presence of space charge formed by the incorporated ions may interact with PAN chains on a microscopic level and may also be distributed according to some non-uniform pattern. The uniformity of any given contribution to the total polarization can be tested by observing how well the behavior of the material conforms to predictions of the "uniform polarization theory" of Bucci, et al<sup>5,6</sup>. This theory gives the temperature-dependence of discharge current as follows:

$$I = \frac{\rho_0}{\tau_0} \exp \left[ -\frac{H}{kT} - (\beta \tau_0)^{-1} \int_{T_0}^T \exp(-\frac{H}{kT}) dT \right] \quad (1)$$

where  $\rho_0 = N\mu^2 E_p^2 / 3kT_p$ ,  $\beta$  is heating rate,  $\tau_0$  is a characteristic relaxation time,  $H$  is energy barrier for the depolarization process to occur,  $k$  is Boltzmann constant,  $T$  is temperature,  $N$  is number of dipoles having a dipole moment,  $\mu$ , per unit volume,  $E_p$  is the electric field used to polarize the specimen at temperature,  $T_p$ . One immediately notes that charge stored by some process having a particular value of  $H$  should be directly proportional to  $E_p$ . Further, a depolarization process can be shown to reach a maximum at a temperature,  $T_{max}$ , that is controlled by a characteristic relaxation time,  $\tau_0$ .  $\tau_0$  is expressed as  $\tau_0 = kT_m^2 / \beta H \exp(H/kT_m)$ ; this shows that  $T_{max}$  should, itself, be independent of both  $E_p$  and  $T_p$ .  $T_{max}$  is also independent of poling time  $t_p$ , at  $T_p$ . It is seen in Table II that discharge maxima at  $-50^\circ C$  conform to these characteristics, while currents discharging at higher temperatures (for example,  $+50^\circ C$ ) fail to do so. Conspicuous departure is seen in the data of Figure 7, where the large  $\beta$  process is seen to exhibit strong dependence on  $T_p$ . Several dispersions have been observed in mechanical and dielectrical measure-

ments in ranges  $50^{\circ}\text{C}$  and lower<sup>12,13</sup>. These dispersions have been attributed to local mode relaxation processes.

Explanation, then, of charge which releases during depolarization at temperatures above  $50^{\circ}\text{C}$  appears to be complicated. Earlier work on undoped PAN<sup>16,17</sup> found the peak near  $95^{\circ}\text{C}$  ( $\gamma_1$ ) to be due to the mechanism of onset of mobility of pendant nitrile dipoles. This peak coincides with the conspicuous maximum in the activation energy spectrum of Figure 5: this peak also corresponds to the abrupt loss of piezoelectricity that has been studied in such ion-doped PAN materials<sup>15</sup>. However, charge released in this temperature range (see Table II) falls considerably short of the upper bound for polarization due to preferential orientation of dipoles, *viz.*,  $14.8 \mu\text{C}/\text{cm}^2$ . In fact, it is known that nitrile dipoles fail to develop preferred orientations close to this upper bound<sup>17</sup>, because very strong dipole-dipole associations successfully prevent a poling field,  $E_p$ , from being able to operate in an uninhibited manner on these dipoles. The observation of this work, however, of an apparent suppression of polarization due to nitrile dipoles is probably evidence for some kind of masking of dipolar polarizations on the microscopic size scale, such as would be represented by a kind of Maxwell-Wagner effect.

A Maxwell-Wagner effect, however, implies the existence of a multi-phase microstructure in the polyacrylonitrile. Slightly different such models have been advanced previously by Miyachi and Andrews<sup>4</sup>, Imai, *et al.*,<sup>10</sup>, Hinrichsen and Orth<sup>18</sup>, and Warner, *et al.*<sup>19</sup>. Each of these models envisions the chain in a more-or-less helical conformation with a lateral packing of the chain segments being fairly close throughout a volume whose characteristic dimensions are on the order of  $100\text{\AA}$ <sup>20</sup>. Thus, the picture may be that two contributions to polarization dominate the depolarization process: the loss of preferred orientation of nitrile dipoles which, in turn, permits the release of masking

charges possibly associated with small ordered domains in PAN.

Charge lost at temperatures above 100°C ( $\beta$  and  $\alpha$  peaks) is ascribed to space charges. The reasons for this assignment are simply the facts that stored charge exceeds by  $10^{+2}$  the upper bound for dipolar polarization and that charging and discharging characteristics, such as  $t_p$ -dependence of  $I_{max}$  and  $T_{max}$  (Figure 7) are unusual. Activation energy for depolarization in this temperature range, as shown in Figure 5, appears actually smaller than that which prevails in the temperature range where depolarization is controlled by dipolar mobility. Activation energies in these high temperature ranges are also smaller than had been reported earlier on undoped PAN<sup>16</sup>. Such a depression of activation energy in the presence of ionic dopants in PAN<sup>21</sup> and other polymers<sup>22</sup> has been reported previously. One can envision that, during the polarization process, ions drift through the bulk material at a rate controlled by the activation energy for transport from site to site. Energetic stability of these sites would vary, depending upon their individual nature. Examples of such lower energy sites, or as they may be called "traps", might be local defects in the chain packing pattern, specific arrangement of nitrile clusters, or interfacial regions between ordered and disordered regions of PAN. The longer the time of polarization, the more a drifting charge should be expected to have encountered an energetically favorable trapping site. It would then follow that depolarization of a specimen polarized for long times would require higher temperatures to achieve discharge than would specimens polarized for short times; this is seen to be the case (see Figure 7).

It is the characteristics, then, of trapped charges that are reflected in TSDC thermograms above 100°C. First of all, the nature of the charge-transporting species needs to be noted. Figure 4 reveals that total charge released by depolarization of space charge is only dependent on ionic con-

centrations below about 1 wt%; above this concentration level there appears to be no further increase in space charge polarization. It seems doubtful to propose that any kind of charge-transfer complex is forming between the polymer and ionic dopant, as had been reported to be the case of Mehendru, et al.,<sup>23</sup> (iodine in polyvinyl acetate) or Shrivastava, et al.<sup>24</sup> (organic molecules in polystyrene). It seems more likely to suppose that such salts as  $\text{NaNO}_3$ , when doped into PAN, have a dissociation constant such that the additional salt above 1 wt% fails to contribute additional ions to the polymer matrix. In exactly what state of aggregation the undissociated  $\text{NaNO}_3$  would be remains undetermined in this study. Free salt ions produced by dissociation should, however, give rise to ionic conductivity, which could be expressed<sup>25</sup> as follows:

$$\sigma = (N_0 v a^2 q / kT) \exp \left\{ -(W+2U) / kT \right\} \quad (2)$$

where  $N_0$  is an adjustable constant,  $v$  is vibrational frequency of a trapped ionic species whose charge is  $q$ ,  $a$  is jump distance for ion moving from site to site,  $W$  is energy for the ion to escape its trap, and  $U$  is the activation energy for transport of the ion through the polymer matrix. The apparent activation energy for this process,  $W+2U$ , can be obtained from the slope of plot,  $\log \sigma T$  vs.  $1/T$ , as is seen in Figure 8. The form of this dependence takes into account the fact that, as temperature rises, both the mobility of the free ions and the population of these charge carriers rise as thermally activated processes. Three distinct rate regions are observed in Figure 8: region I is characterized by very low conductivities, which can be interpreted as meaning extremely low population of charge carriers whose transport activation energy is also somewhat small. Region II shows a very rapid rise and conductivity, coincident with the  $\gamma$  peaks (whose origin has been ascribed to the onset of chain segmental mobility). The final region, III, shows a

continued rise in  $\sigma T$ , but with a progressively declining slope. This is in agreement with the falloff in TSDC activation energy,  $H$ , seen in Figure 5. Yet, the large increases associated with the incorporation of ions (lines b and c) due to the incorporation of ionic species clearly indicates that the population of ionic charge carriers, and especially the temperature-dependence of this population, must have its effect on the charge transport process. To any extent that there is structure left in the packing of PAN chains, as has been discussed previously in terms of ordering in PAN, then one might expect the discharging of the  $\alpha$  and  $\beta$  polarization contributions to reflect some Maxwell-Wagner polarization effects, as well.

The dielectric relaxation time,  $\tau$ , for such effects is determined by equation 3:

$$\tau = (2\epsilon_1 + \epsilon_2)/4\pi(2\sigma_1 + \sigma_2) \quad (3)$$

where  $\epsilon$ 's are dielectric constants and  $\sigma$ 's are conductivities, 1's denote the phase dispersed in the matrix whose subscript is 2. Figure 9 shows the temperature-dependence of low frequency (11 Hz) dielectric constant. The rise in apparent dielectric constant above  $50^\circ$  is exactly coincident with the region II of the conductivity data (Figure 8). Incorporation of ionic species into the PAN greatly magnifies this effect by nearly 3 orders of magnitude by the time temperature has risen to  $150^\circ$ C. Since dielectric constants are not likely to change by such huge factors over that temperature range, then the effect must be ascribed almost exclusively to increases in charge transport, as embraced by the conductivity parameter,  $\sigma$ . This further underscores the assignment of space charge relaxations to the  $\alpha$  and  $\beta$  peaks seen in the TSD thermograms of ion-doped PAN.

### CONCLUSIONS

Thermally Stimulated Discharge Currents of  $\text{NaNO}_3$ -doped films show at least five remarkable peaks: around  $170^\circ\text{C}(\alpha)$ ,  $160\text{-}100^\circ\text{C}(\beta)$ ,  $70^\circ\text{C}(\gamma_2)$ ,  $50^\circ\text{C}(\gamma_3)$  and  $-50^\circ\text{C}(\delta)$ .  $\beta$  peak temperatures ( $T_{\max}$ ) and peak currents ( $I_{\max}$ ) are dependent upon the ion concentration and poling time, so it is proposed that this peak might be associated with Maxwell-Wagner type polarization involving space charges and the inhomogeneous structure of PAN. The  $I_{\max}$  of both  $\gamma_2$  and  $\gamma_3$  are also strongly dependent upon  $\text{NaNO}_3$  concentration and poling time, and these peak currents are also dependent upon which ionic species, specifically  $\text{NaNO}_3$ ,  $\text{NH}_4\text{NO}_3$ , or  $\text{LiCl}$ , are present. The  $\gamma_3$  peak may arise from space charges that release following the onset of some local mode molecular motion in PAN.

From both dc electrical conductivity measurement and from TSDC analysis, it is confirmed that a glass-rubber transition temperature (around  $95^\circ\text{C}$ ) is not appreciably shifted by  $\text{NaNO}_3$  doping to levels employed in this study. This result suggests that the interaction between  $\text{NaNO}_3$  and PAN chains, as whole entities themselves, is not very strong.

### ACKNOWLEDGEMENTS

The authors are indebted to the Office of Naval Research for its generous support of this project. Use of the Central Facilities of Northwestern University's Materials Research Center, presently supported under the NSF-MRL program grant DMR79-23573, facilitated much of the experimentation.

REFERENCES

1. M. Kawai, Jpn. J. Appl. Phys., 8, 975 (1969).
2. A. E. Woodward, J. M. Crissman and J. A. Sauer, J. Polym. Sci., 44, 23 (1960).
3. C. W. Deeley, A. E. Woodward and J. A. Sauer, J. Appl. Phys., 28, 1124 (1957).
4. K. Miyachi and R. D. Andrews, Appl. Polym. Symp. No. 25, 127 (1974).
5. C. Bucci and R. Fieschi, Phys. Rev. Lett., 12, No. 1, 16 (1964).
6. C. Bucci, R. Fieschi and G. Guidi, Phys. Rev., 148, No. 2, 816 (1966).
7. M. M. Perlman, J. Appl. Phys., 42, No. 2, 531 (1971); J. Appl. Phys., 42, No. 7, 2645 (1971).
8. J. van Turnhout, Polym. J., 2, 173 (1971).
9. T. Takamatsu and E. Fukada, Polym. J., 1, 101 (1970).
10. Y. Imai, S. Minami, T. Yashihara, Y. Joh and H. Sato, Polymer Letters, 8, 281 (1970).
11. S. Minami, T. Yashihara and H. Sato, Kobunshi Kagaku, 1, 125 (1972).
12. Y. Ishida, M. Matsuo, Y. Ueno and M. Takayanagi, Kolloid-Z.Z. Polym., 199, 67 (1964).
13. L.K.H. Van Beek, J. Appl. Polym. Sci., 9, 553 (1965).
14. R. Hayakana, T. Nishi, K. Arisawa and Y. Wada, J. Polym. Sci., A2, 5, 165 (1967).
15. H. Ueda and S. H. Carr, to be published.
16. R. J. Comstock, S. I. Stupp and S. H. Carr, J. Macromol. Sci.-Phys., B13, (1), 101 (1977).
17. S. I. Stupp and S. H. Carr, J. Polym. Sci., Polym. Phys. Ed., 16, 13 (1978).
18. G. Hinrichsen and H. Orth, Polym. Letters, 9, 529 (1971).
19. S. B. Warner, L. H. Peebles, Jr., D. R. Uhlmann, Office of Naval Research, Technical Report No. 1, for Contract N00014-75-C-0542 (1978).

20. G. Hinrichsen, J. Polym. Sci., Part C, No. 38, 303 (1972).
21. S. Reich and I. Michaeli, J. Polym. Sci.-Polym. Phys. Ed., 13, 19 (1975).
22. K. F. Wissbrun and M. J. Hannon, J. Polym. Sci., Polym. Phys. Ed., 13, 223 (1975).
23. P. C. Mehendru, K. Jain and Praveen Mehendru, J. Phys. D; Appl. Phys. 9, 83 (1974).
24. S. K. Shrivastava, J. D. Ranade and A. P. Shrivastava, Physics Letters, 69A, 465 (1979).
25. R. E. Barber, Jr. and C. R. Thomas, J. Appl. Phys., 35, No. 11, 3203 (1964).

Table I

Depolarization Charge.  $\left[ \text{Coulomb-cm}^{-2} \right]$

	$\delta$	$\gamma_3$	$> 70^\circ\text{C}$
LiCl	$6.2 \times 10^{-9}$	$20 \times 10^{-8}$	$13 \times 10^{-4}$
$\text{NaNO}_3$	$7.2 \times 10^{-9}$	$20 \times 10^{-8}$	$11 \times 10^{-4}$
$\text{NH}_4\text{NO}_3$	$6.0 \times 10^{-9}$	$2.8 \times 10^{-8}$	$1.5 \times 10^{-4}$

Salt conc.,  $C = 2 \times 10^{-5}$  mol/PAN gr.

Poling Field,  $E_p = 5 \times 10^4$  V/cm<sup>-1</sup>

Table II

$E_p (10^4 \text{V/cm})$	I at $-50^\circ\text{C}$ (A)		I at $50^\circ\text{C}$ (A)	
	$C = 1 \times 10^{-4}$	$C = 2 \times 10^{-4}$ (mole/grPAN)	$C = 1 \times 10^{-4}$	$C = 2 \times 10^{-4}$
5	$1.8 \times 10^{-11}$	$1.9 \times 10^{-11}$	$6.4 \times 10^{-9}$	$2.6 \times 10^{-9}$
10	$4.0 \times 10^{-11}$	$3.9 \times 10^{-11}$	$8.9 \times 10^{-9}$	$1.1 \times 10^{-9}$

$1 \times 10^{-4}$   $\text{NaNO}_3$  mole/grPAN) = 0.85 wt% salt

$1 \times 10^{-4}$   $\text{NaNO}_3$  mole/grPAN) =  $5.3 \times 10^{-3}$  mol/AN residue

FIGURE CAPTIONS

**Figure 1.** Thermally stimulated depolarization current from  $\text{NaNO}_3$ -doped polyacrylonitrile polarized under a field of  $5 \times 10^{-4}$  V/cm at  $130^\circ\text{C}$  for 30 min. Heating rate was  $2^\circ\text{C}/\text{min}$ . Concentrations in mole/gmPAN are a = pure film, b =  $1 \times 10^{-5}$ , c =  $5 \times 10^{-5}$ , d =  $1 \times 10^{-4}$ , e =  $5 \times 10^{-4}$ .

**Figure 2.** Thermally stimulated depolarization currents from  $\text{NaNO}_3$ -doped polyacrylonitrile polarized under a field of  $5 \times 10^{-4}$  V/cm at  $130^\circ\text{C}$  for 30 min. Concentrations in mole/gmPAN are a = pure, b =  $1 \times 10^{-6}$ , c =  $1 \times 10^{-5}$ , d =  $2 \times 10^{-5}$ , e =  $5 \times 10^{-5}$ , f =  $1 \times 10^{-4}$ , g =  $5 \times 10^{-4}$ .

**Figure 3.** Concentration-dependence of TSDC peaks,  $T_{\max}$ 's, seen in thermograms of Figures 1 and 2.

**Figure 4.** The relation between thermally stimulated depolarization charges, Q, that release above  $70^\circ\text{C}$  and  $\text{NaNO}_3$  concentration (wt%) in polyacrylonitrile that had been polarized at  $130^\circ\text{C}$  under a field of  $5 \times 10^{-4}$  V/cm for 30 min.

**Figure 5.** Apparent activation energies from partial heating experiments in pure polyacrylonitrile film (0) and in  $\text{NaNO}_3$ -doped film ( $2 \times 10^{-5}$  mole/gmPAN) ( $\Delta$ ).

**Figure 6.** Thermally stimulated depolarization currents for  $\text{NH}_4\text{NO}_3$ -doped (N) and LiCl-doped (L) polyacrylonitrile polarized a field of  $5 \times 10^{-4}$  V/cm at  $130^\circ$  for 30 min. N-1 =  $2 \times 10^{-5}$  mole  $\text{NH}_4\text{NO}_3$ /gmPAN; N-2 =  $2 \times 10^{-4}$  mole  $\text{NH}_4\text{NO}_3$ /gmPAN; L-1 =  $2 \times 10^{-5}$  mole LiCl/gmPAN; L-2 =  $2 \times 10^{-4}$  mole LiCl/gmPAN.

Figure 7. Thermally stimulated depolarization currents for  $\text{NaNO}_3$ -doped polyacrylonitrile ( $2 \times 10^{-5}$  mole/gmPAN) polarized a field of  $5 \times 10^4$  V/cm for 30 min. (a) and for 120 min. (b).

Figure 8. Temperature-dependence of the second run of dc conductivity (cooled after the first measurement under an applied field) for  $\text{NaNO}_3$ -doped and undoped polyacrylonitrile, measured at heating rate of  $2^\circ\text{C}/\text{min}$ . Concentrations in mole/gmPAN are a = pure, b =  $2 \times 10^{-5}$ , b' =  $2 \times 10^{-5}$  ( $\text{NH}_4\text{NO}_3$ -doped PAN), c =  $5 \times 10^{-4}$  [mole/gmPAN]. Doped specimens were poled under an electrical field of  $5 \times 10^3$  V/cm, and undoped films were poled using  $1 \times 10^4$  V/cm.

Figure 9. Temperature-dependence of dielectric constant ( $\epsilon$ ) for  $\text{NaNO}_3$ -doped polyacrylonitrile measured at 11 Hz. Concentrations in mole/gm PAN are a = pure, b =  $1 \times 10^{-5}$ , c =  $5 \times 10^{-5}$ , d =  $1 \times 10^{-4}$ , e =  $2 \times 10^{-4}$ .

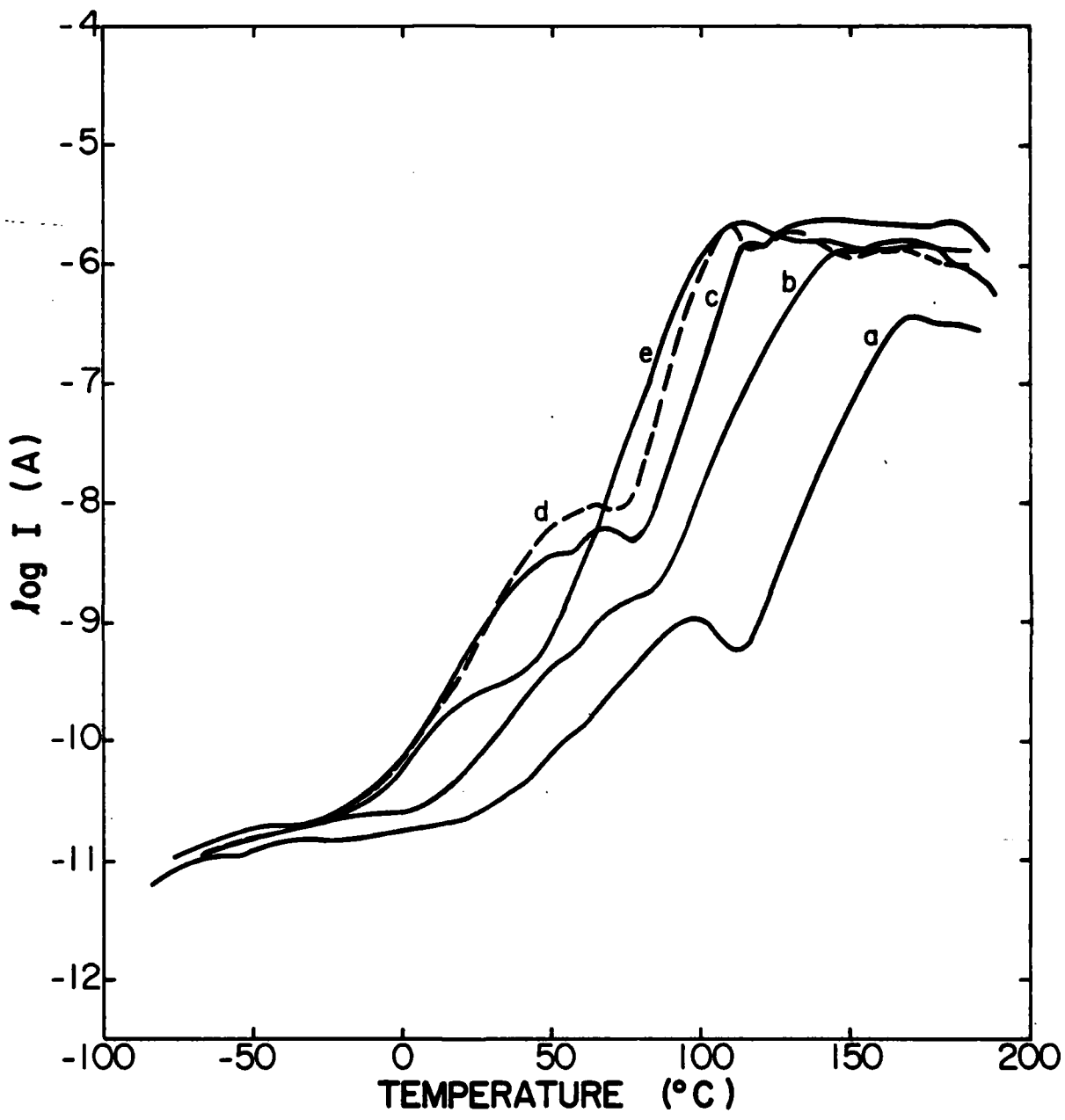


Figure 1.

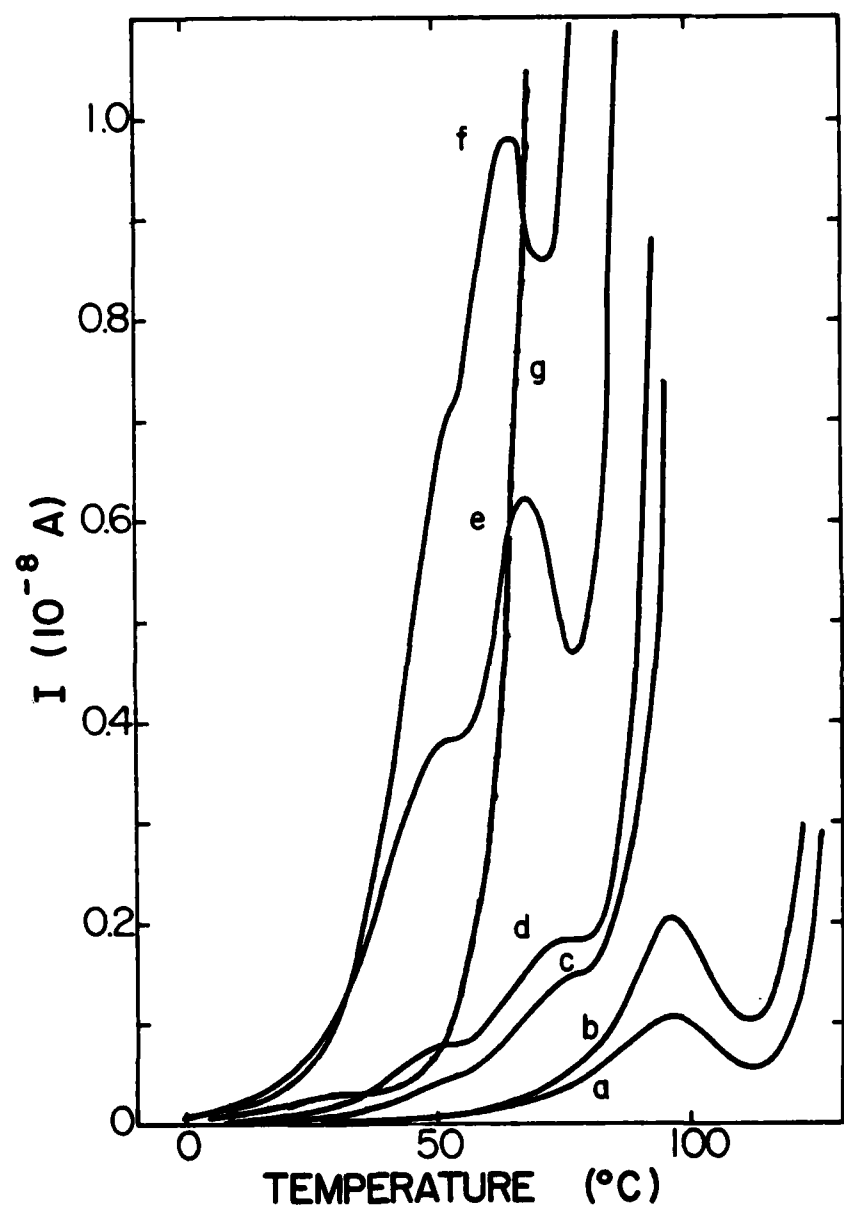


Figure 2.

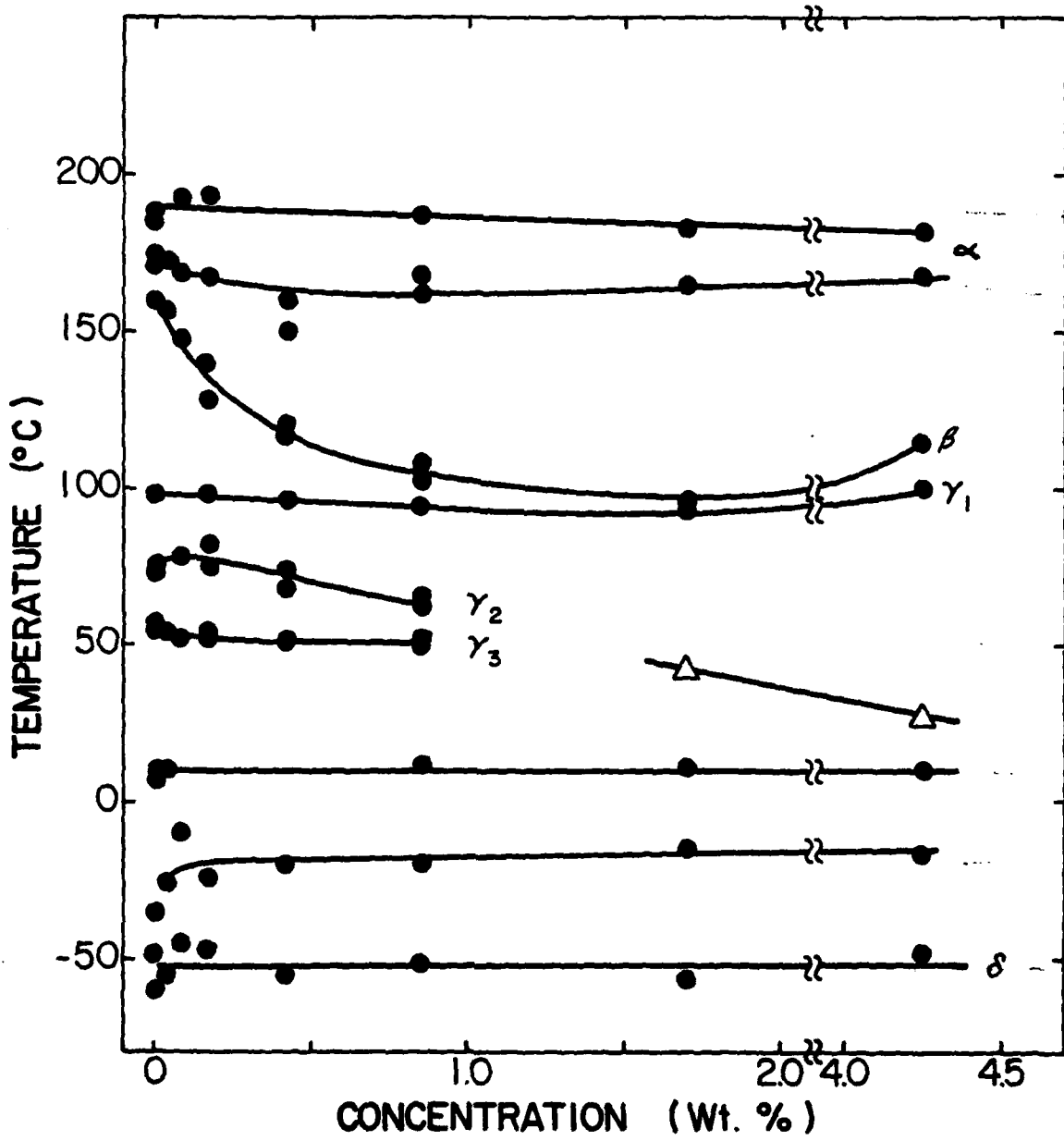


Figure 3.

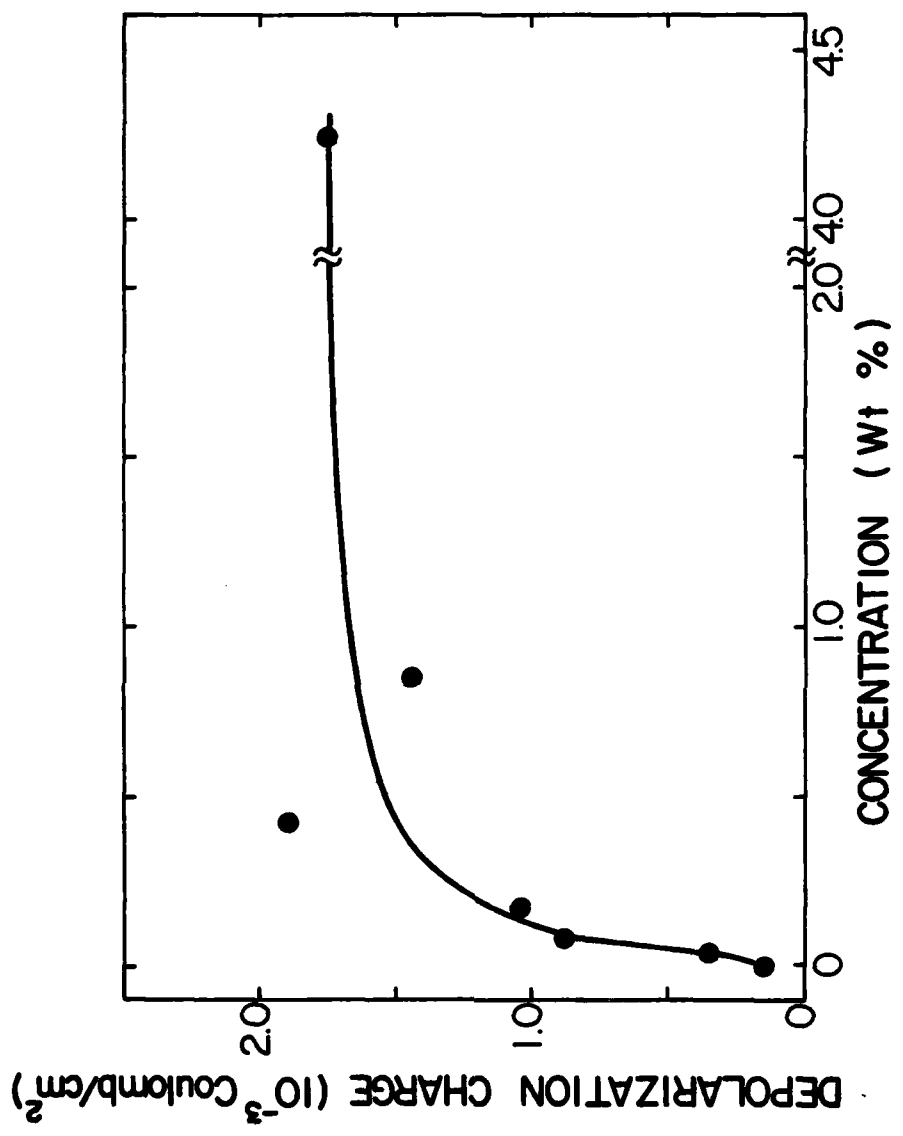


Figure 4.

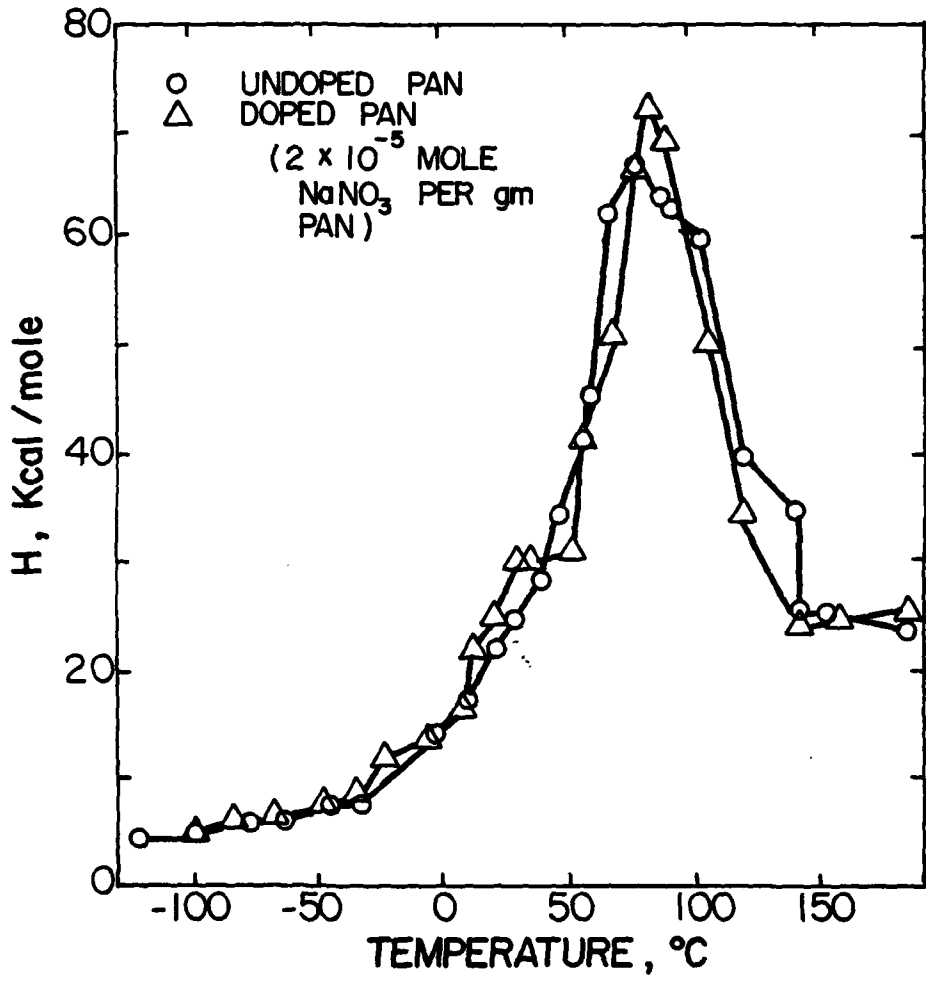


Figure 5.

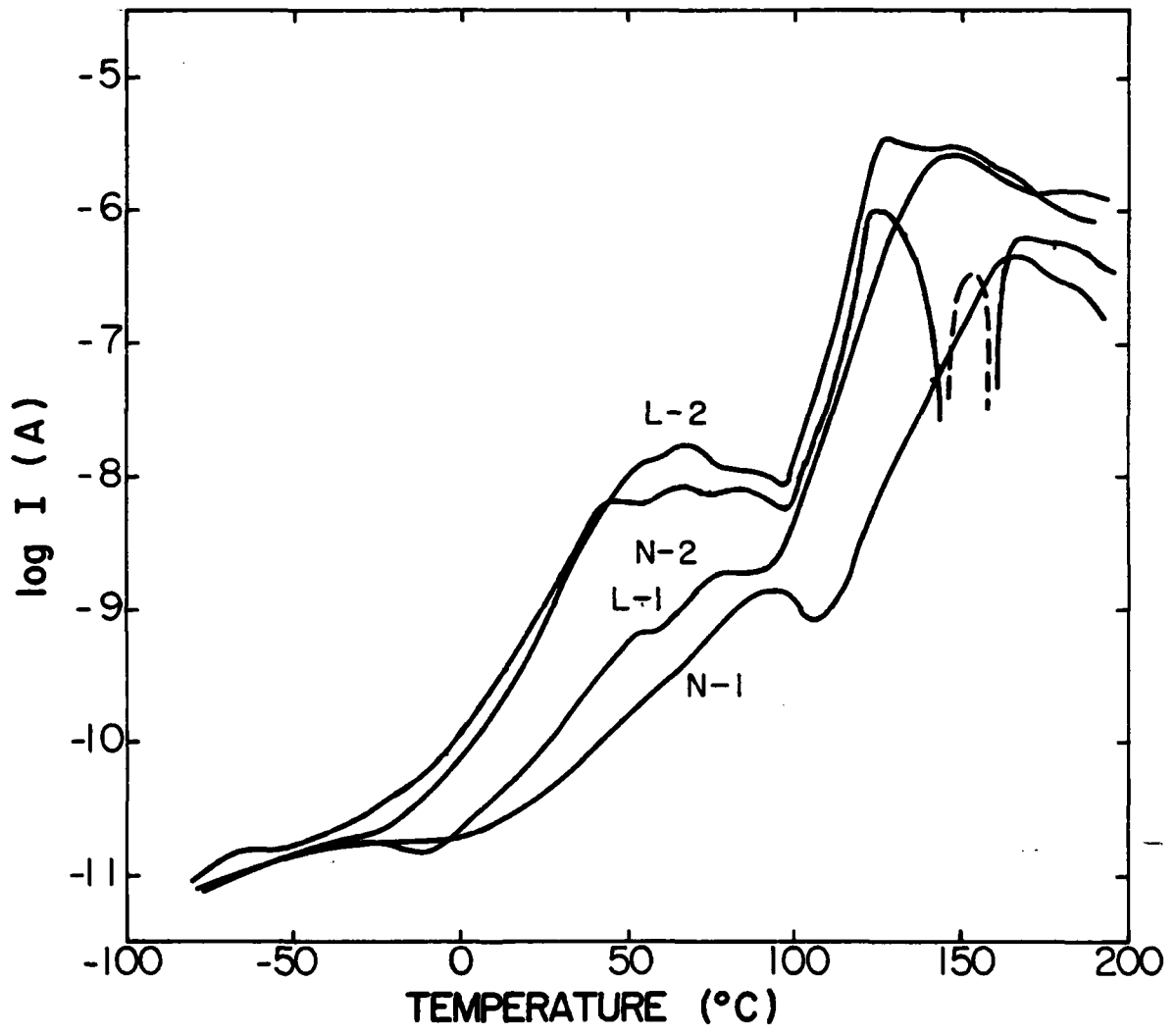


Figure 6.

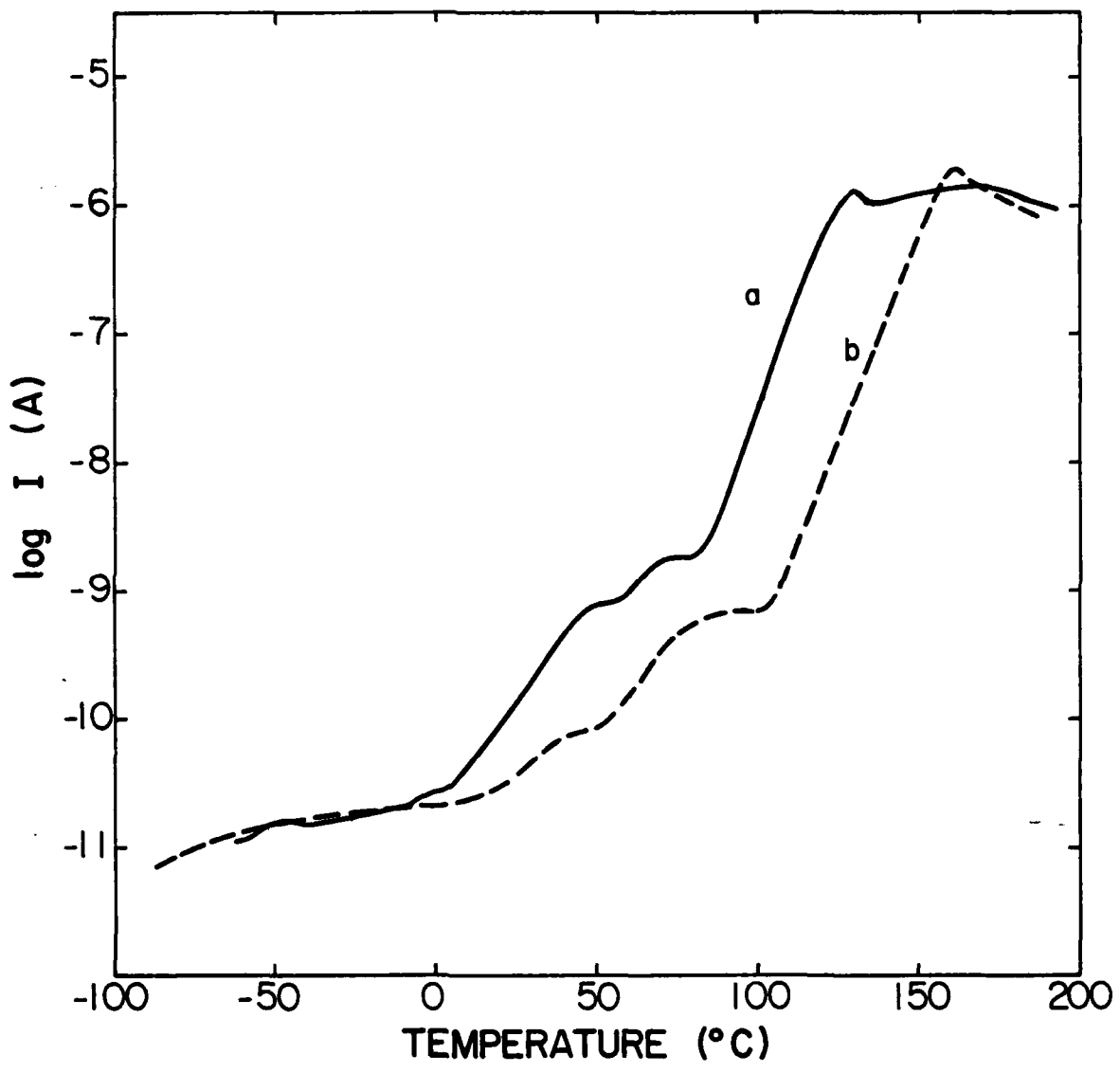


Figure 7.

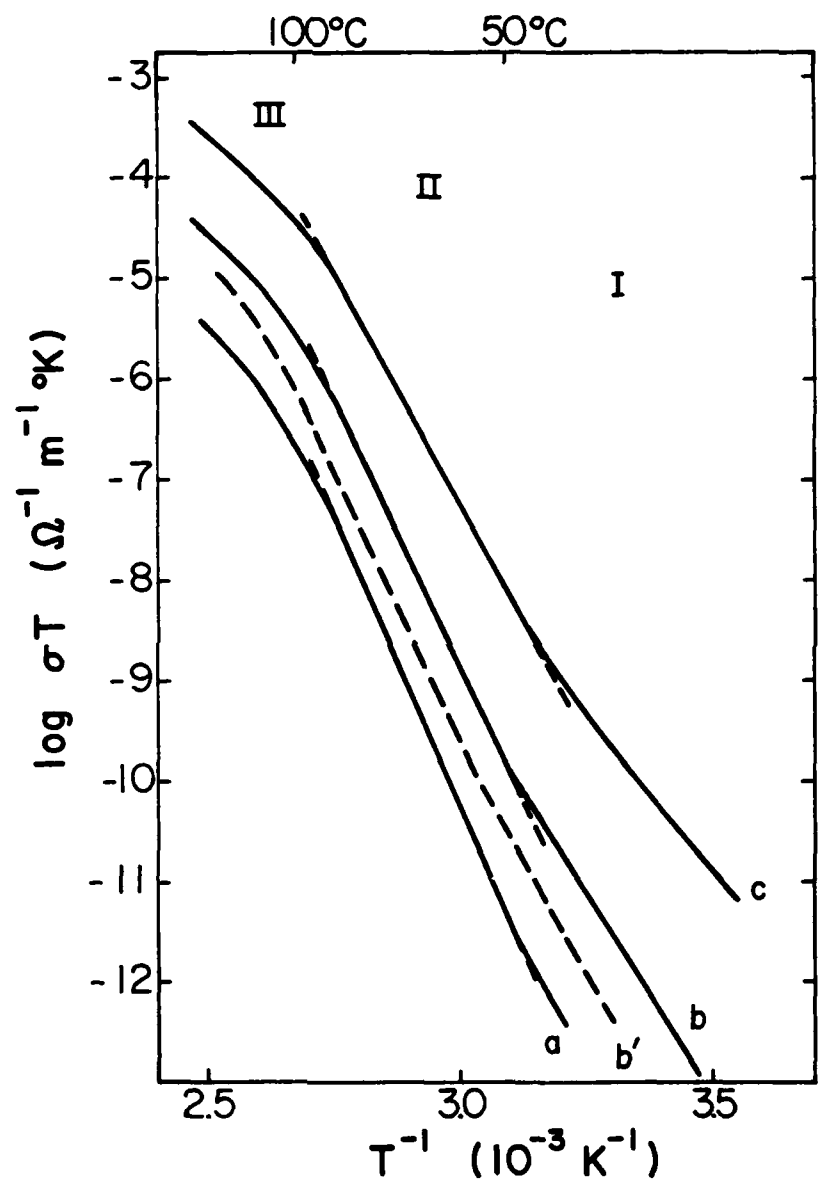


Figure 8.

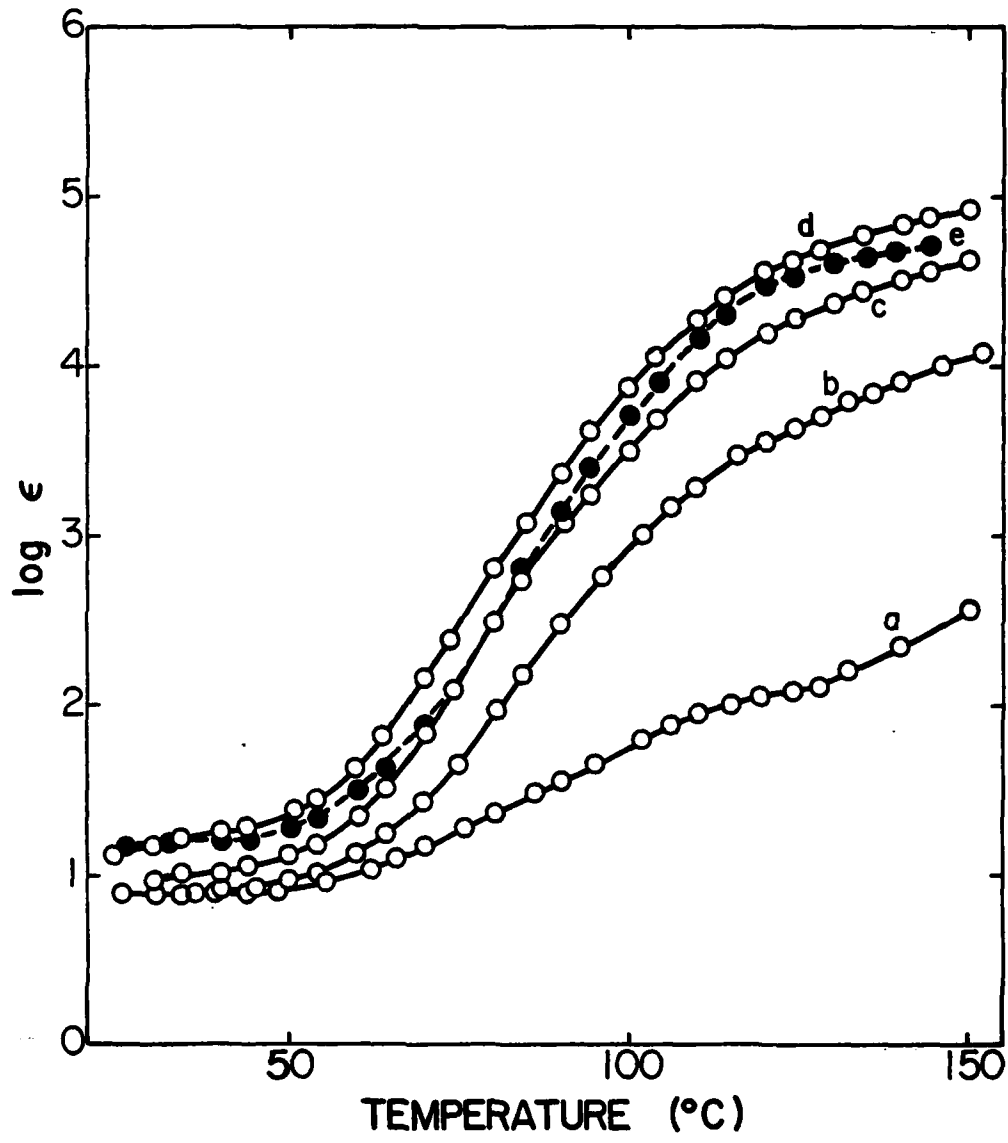


Figure 9.

TECHNICAL REPORT DISTRIBUTION LIST, 356A

<u>No.</u>	<u>Copies</u>	<u>No.</u>	<u>Copies</u>
Mr. L. A. Smith Singer Aerospace Kearfett Division 1150 McBride Avenue Little Falls, NJ 07424	1	Picatinny Arsenal SMUPA-FR-M-D Dover, New Jersey 07801 Attn: A. M. Anzalone Building 3401	1
Dr. M. Broadhurst Bulk Properties Section National Bureau of Standards U.S. Department of Commerce Washington, D.C. 20234	2	Dr. J. K. Gillham Princeton University Department of Chemistry Princeton, New Jersey 08540	1
Dr. T. A. Litovitz Department of Physics Catholic University of America Washington, D.C. 20017	1	Douglas Aircraft Co. 3855 Lakewood Boulevard Long Beach, California 90846 Attn: Technical Library CI 290/36-84 AUTO-Sutton	1
Dr. R. V. Subramanian Washington State University Department of Materials Science Pullman, Washington 99163+	1	Dean Eric Baer School of Engineering Case Institute of Technology Case Western Reserve University Cleveland, OH 44106	1
Dr. M. Shen Department of Chemical Engineering University of California Berkeley, California 94720	1	Dr. K. D. Pae Department of Mechanics and Materials Science Rutgers University New Brunswick, New Jersey 08903	1
Dr. V. Stannett Department of Chemical Engineering North Carolina State University Raleigh, North Carolina 27607	1	NASA-Lewis Research Center 21000 Brookpark Road Cleveland, Ohio 44135 Attn: Dr. T. T. Serofini, MS-49-1	1
Dr. D. R. Uhlmann Department of Metallurgy and Material Science Center for Materials Science and Engineering Massachusetts Institute of Technology Cambridge, Massachusetts 02139	1	Dr. Charles H. Sherman, Code TD 121 Naval Underwater Systems Center New London, Connecticut 06320	1
Naval Surface Weapons Center White Oak Silver Spring, Maryland 20910 Attn: Dr. J. M. Augl Dr. B. Hartman	1	Dr. William Risen Department of Chemistry Brown University Providence, Rhode Island 02192	1
Dr. S. Goodman Globe Union Incorporated 5757 North Green Bay Avenue Milwaukee, Wisconsin 53201	1	Dr. Alan Gent Department of Physics University of Akron Akron, Ohio 44304	1

• 1 / 75

472:CAN:716:tam  
78w472-608

TECHNICAL REPORT DISTRIBUTION LIST, GEN

	<u>No. Copies</u>	<u>No. Copies</u>
Office of Naval Research 800 North Quincy Street Arlington, Virginia 22217 Attn: Code 472	2	Defense Documentation Center Building 5, Cameron Station Alexandria, Virginia 22314
ONR Branch Office 536 S. Clark Street Chicago, Illinois 60605 Attn: Dr. George Sandoz	1	U.S. Army Research Office P.O. Box 1211 Research Triangle Park, N.C. 27709 Attn: CRD-AA-IP
ONR Branch Office 715 Broadway New York, New York 10003 Attn: Scientific Dept.	1	Naval Ocean Systems Center San Diego, California 92152 Attn: Mr. Joe McCartney
ONR Branch Office 1030 East Green Street Pasadena, California 91106 Attn: Dr. R. J. Marcus	1	Naval Weapons Center China Lake, California 93555 Attn: Dr. A. B. Amster Chemistry Division
ONR Area Office One Hallidie Plaza, Suite 601 San Francisco, California 94102 Attn: Dr. P. A. Miller	1	Naval Civil Engineering Laboratory Port Hueneme, California 93401 Attn: Dr. R. W. Drisko
ONR Branch Office Building 114, Section D 666 Summer Street Boston, Massachusetts 02210 Attn: Dr. L. H. Peebles	1	Professor K. E. Woehler Department of Physics & Chemistry Naval Postgraduate School Monterey, California 93940
Director, Naval Research Laboratory Washington, D.C. 20390 Attn: Code 6100	1	Dr. A. L. Slafkosky Scientific Advisor Commandant of the Marine Corps (Code RD-1) Washington, D.C. 20380
The Assistant Secretary of the Navy (R,E&S) Department of the Navy Room 4E736, Pentagon Washington, D.C. 20350	1	Office of Naval Research 800 N. Quincy Street Arlington, Virginia 22217 Attn: Dr. Richard S. Miller
Commander, Naval Air Systems Command Department of the Navy Washington, D.C. 20360 Attn: Code 310C (H. Rosenwasser)	1	Naval Ship Research and Development Center Annapolis, Maryland 21401 Attn: Dr. G. Bosmajian Applied Chemistry Division
	1	Naval Ocean Systems Center San Diego, California 92132 Attn: Dr. S. Yamamoto, Marine Sciences Division

Enel |

TECHNICAL REPORT DISTRIBUTION LIST, 356A

<u>No.</u> <u>Copies</u>	<u>No.</u> <u>Copie</u>		
Mr. Robert W. Jones Advanced Projects Manager Hughes Aircraft Company Mail Station D 132 Culver City, California 90230	1	Dr. T. J. Reinhart, Jr., Chief Composite and Fibrous Materials Branch Nonmetallic Materials Division Department of the Air Force Air Force Materials Laboratory (AFSC) Wright-Patterson Air Force Base, Ohio 454	1
Dr. C. Giori IIT Research Institute 10 West 35 Street Chicago, Illinois 60616	1	Dr. J. Lando Department of Macromolecular Science Case Western Reserve University Cleveland, Ohio 44106	1
Dr. M. Litt Department of Macromolecular Science Case Western Reserve University Cleveland, Ohio 44106	1	Dr. J. White Chemical and Metallurgical Engineering University of Tennessee Knoxville, Tennessee 37916	1
Dr. R. S. Roe Department of Materials Science and Metallurgical Engineering University of Cincinnati Cincinnati, Ohio 45221	1	Dr. J. A. Manson Materials Research Center Lehigh University Bethlehem, Pennsylvania 18015	1
Dr. L. E. Smith U.S. Department of Commerce National Bureau of Standards Stability and Standards Washington, D.C. 20234	1	Dr. R. F. Helmreich Contract RD&E Dow Chemical Co. Midland, Michigan 48640	1
Dr. Robert E. Cohen Chemical Engineering Department Massachusetts Institute of Technology Cambridge, Massachusetts 02139	1	Dr. R. S. Porter University of Massachusetts Department of Polymer Science and Engineering Amherst, Massachusetts 01002	1
Dr. David Roylance Department of Materials Science and Engineering Massachusetts Institute of Technology Cambridge, Massachusetts 02039	1	Professor Garth Wilkes Department of Chemical Engineering Virginia Polytechnic Institute and State University Blacksburg, Virginia 24061	1
Dr. T. P. Conlon, Jr., Code 3622 Sandia Laboratories Sandia Corporation Albuquerque, New Mexico 87115	1	Dr. Kurt Baum Fluorochem Inc. 6233 North Irwindale Avenue Azusa, California 91702	1
Dr. Martin Kaufmann, Head Materials Research Branch, Code 4542 Naval Weapons Center China Lake, California 93555	1	Professor C. S. Paik Sung Department of Materials Sciences and Engineering Massachusetts Institute of Technology Cambridge, Massachusetts 02139	2